Progress In Electromagnetics Research M, Vol. 121, 117–125, 2023

An Ultra-Wideband and Translucent Metasurface Absorber Based on Water

Chaobiao Chen[1], Tianhang Chen[2], Min Huang[1, *], Huan Lu[1], and Bin Zheng[1, *]

Abstract—Electromagnetic metasurface has become the focus of researchers in the field of electromagnetic absorption in recent years because of its thin thickness, simple structure, and high absorption rate. With high real and imaginary parts of the permittivity in the microwave frequency regime, water plays a crucial role in absorbing materials. This work demonstrates a water-based translucent metasurface with 5.2 mm, which is fabricated by 3D printing. By changing the conductivity of water, a metasurface with good absorption performance is obtained, which can realize ultra-wideband absorption in 5.85–23.1 GHz and 5.85–14.8 GHz under the oblique incidence of 40°. The metasurface has the characteristics of thin thickness, wide-band absorption, and translucency.

1. INTRODUCTION

Electromagnetic (EM) absorptive materials have wide application prospects in EM energy harvesting [1], detection [2–4], and focusing [5–8] due to their effective absorption of incident EM waves. EM absorptive materials can not only provide solutions for stealth technology and EM compatibility [9–11], but also be used to suppress EM radiation pollution and anti-microwave interference [12–15]. Metasurfaces formed by subwavelength metal structures arranged on the substrate in a periodic or regular aperiodic manner have great potential in applying metamaterial absorbers due to the high loss generated by resonant structures. Classical EM absorptive materials such as Salisbury screen [16], Jauman absorbers [17], and Dallenbach absorbers [18] have the disadvantages of large volume and narrow bandwidth. Because of the high resonance dispersion of metal, it is challenging to achieve broadband absorption for monolayer metamaterials. Broadband absorption can be realized by stacking multilayer structures and loading lumped resistors [19], but they increase the thickness of the metamaterial. It remains a challenge to achieve broadband absorption at the thin thickness of metamaterials.

Liquid can not only serve as the substrate of metamaterial, but also form a three-dimensional structure surrounded by substrate, which can realize microwave absorption [20–24]. These metamaterials that contain liquids are called liquid metamaterials. There are many types of liquid in liquid metamaterials, including water [25–27], ethanol [28], liquid metals [29], liquid crystals [30], etc. Water is widely used in liquid metamaterials because of its non-polluting, low cost, and easy availability [31]. Due to the large imaginary part of the permittivity of water, the water-based metamaterial is considered a good absorber in the microwave frequency regime [32–36]. Reference [37] presents a water-substrate metasurface absorber with a metal fishbone structure, which can achieve broadband absorption from 2.6 GHz to 16.8 GHz and has a thickness of 15 mm. Reference [38] presents an ultra-wideband metamaterial absorber with over 90% absorptivity from 12 GHz to 29.6 GHz, and its

Received 6 August 2023, Accepted 9 November 2023, Scheduled 27 November 2023

* Corresponding authors: Min Huang (12031022@zju.edu.cn), Bin Zheng (zhengbin@zju.edu.cn).

[1] Interdisciplinary Center for Quantum Information, State Key Laboratory of Modern Optical Instrumentation, ZJU-Hangzhou Global Scientific and Technological Innovation Center, Zhejiang University, Hangzhou 310027, China. [2] International Joint Innovation Center, Key Lab. of Advanced Micro/Nano Electronic Devices & Smart Systems of Zhejiang, The Electromagnetics Academy at Zhejiang University, Zhejiang University, Haining 314400, China. [3] Jinhua Institute of Zhejiang University, Zhejiang University, Jinhua 321099, China. [4] China Aeronautical Establishment, Beijing 100029, China.

thickness is 5.8 mm. In [39], a water-injected metamaterial absorber is presented, which can realize an absorption over 90% in the range of 8.1–22.9 GHz. Reference [40] presents a transparent water-based metamaterial absorber with high absorption over 90% at 13.3–40 GHz, and its thickness is 15 mm. These absorbers have the disadvantages of thick thickness and no absorption at low frequency regime.

In this work, water and salt solution of different concentrations was selected as absorbing materials, and transparent photosensitive resin (Somos WaterClear Ultra 10122) was used to fix the water structure and as a container. In the second section, the design of a translucent water-based metasurface is presented, and the design process is introduced in detail. Then, the simulation results are given in the third section. The structural parameters are optimized, and we discuss the simulation results. In the fourth section, the experimental results are carried out, and the processing methods are described. Finally, we conclude the salt solution concentration with the best absorption according to the experimental results.

2. DESIGN OF TRANSLUCENT WATER-BASED METASURFACE

The water-resonator-based metasurface is illustrated in Fig. 1. The blue structure is water resonant structure, and the yellow structure is substrate. It can be seen that the water resonance structure consists of a bottom square ring and four cuboids. The design of the square ring is inspired by the metal square ring metamaterial, whose strong resonance in the low frequency regime enables the metamaterial to have strong absorption in the low frequency regime. The cuboid is placed above the square ring to broaden the absorption bandwidth. In order to make the overall structure remain polarized independent, four cuboids need to be placed above the square ring. Due to the fluidity of water, the water resonant structure is surrounded by the yellow substrate, as shown in Figs. 1(b), 1(c) and 1(d). The resonant peak can be changed to adjust the microwave absorption by adjusting the parameters of square rings

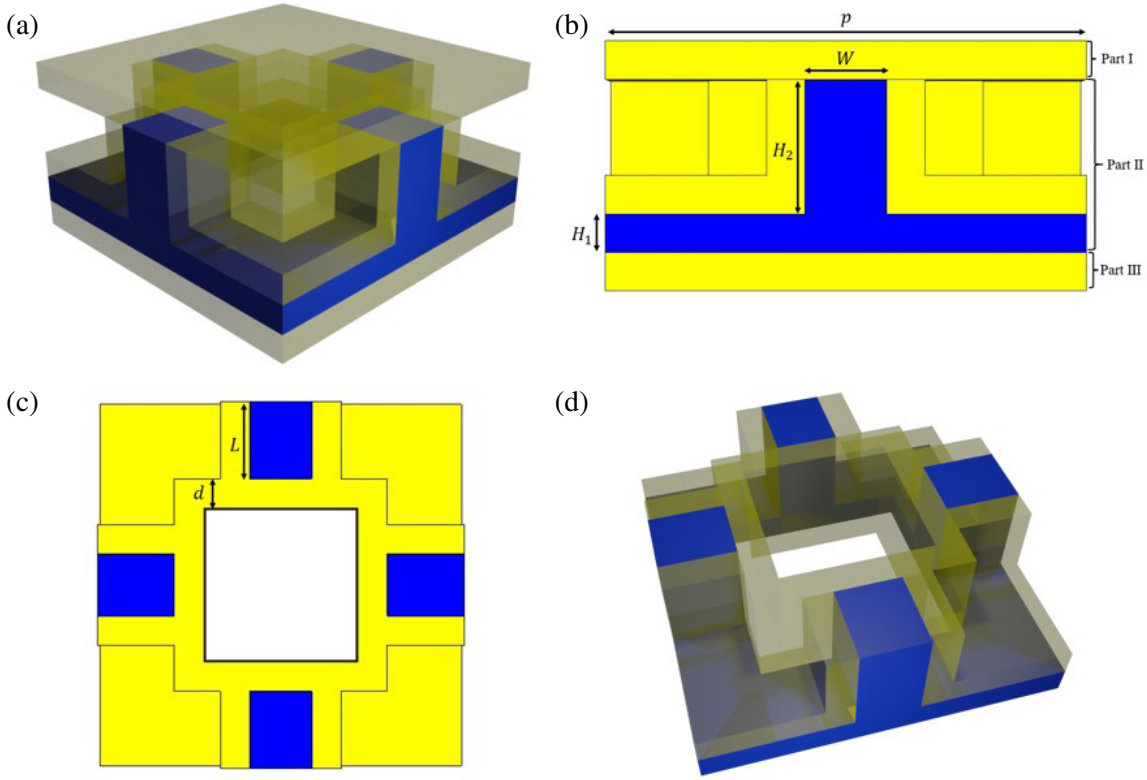

Figure 1. (a) Schematic of the translucent water-based metasurface. (b) Side view of the translucent water-based metasurface. (c) Top view of part II. (d) Schematic of part II.

and cuboids. Since the square ring and four cuboids are connected, the water resonance structure can be filled by reserving one water inlet and one water outlet in the overall structure. The substrate is Somos WaterClear Ultra 10122 (SWU10122), which has a relative permittivity of 2.8 in the microwave frequency regime. SWU10122 is an optically transparent 3D printing material that produces colourless parts that mimic the appearance of acrylic acid.

3. NUMERICAL ANALYSIS

As the water resonant structure of translucent water-based metasurface, the square ring and four cuboids, which are surrounded by the substrate to form a designed fixed structure, can generate several resonant frequencies. Due to the high real part of the permittivity of water, an EM resonance is excited at certain frequencies in the water resonant structure designed by specific geometric parameters. In addition, the high imaginary part of the permittivity of water in the microwave frequency range enables the water resonant structure to carry out wideband absorption near the resonant frequency. CST simulation software was used to simulate the cell structure. The permittivity of distilled water can be described by the Debye model [41], which can be found in the material library in the CST software. The simulation results are shown in Fig. 2 when the geometric parameters of translucent water-based metasurface are finally determined to be $W = 1.7\,\text{mm}$, $L = 2.1\,\text{mm}$, $H_1 = 0.8\,\text{mm}$, $H_2 = 2.8\,\text{mm}$, $d = 0.8\,\text{mm}$, $p = 10\,\text{mm}$. In addition, the thickness of all substrates is 0.8 mm, and the total thickness of the metasurface is 5.2 mm. Considering that the cell structure is completely symmetric, it can be concluded that the reflection of the incident of the polarized EM wave in the y-direction is the same as x-direction.

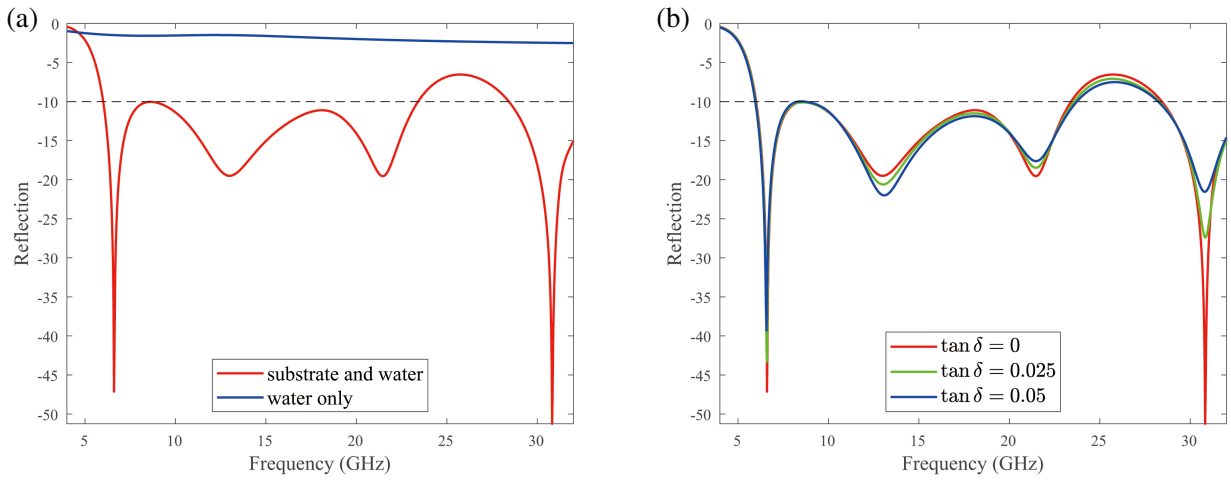

Figure 2. (a) Reflection of cell structure which consist of only water and consist of both substrate and water. (b) Reflection of cell structure when the value of substrate loss tangent is 0, 0.025 and 0.05.

As shown in Fig. 2(a), there are three resonant frequencies in the frequency regime with reflection less than $-10\,\text{dB}$, which are $f_{TE1} = f_{TM1} = 6.6\,\text{GHz}$, $f_{TE2} = f_{TM2} = 13\,\text{GHz}$, and $f_{TE3} = f_{TM3} = 21.5\,\text{GHz}$. The power loss density of these six resonant frequencies is shown in Fig. 3. The resonant frequencies f_{TE1} and f_{TM1} are contributed by the water square ring. The resonant frequencies f_{TE2} and f_{TM2} are mainly contributed by the lower half of the water cuboid, and the resonant frequencies f_{TE3} and f_{TM3} are mainly contributed by the upper half of the water cuboid. The incident EM wave has no power loss on the substrate, so it seems that the substrate has no effect in the metasurface. All the substrate in Fig. 1(a) is replaced with water to find out the effect of the substrate on reflection. The reflection of a metasurface consisting of only water is shown in Fig. 2(a). When the metasurface is composed of only water, the reflection is almost 0 dB. That is, there is no absorption. Thus, the substrate is not only to surround the water resonant structure, but also to make it form an impedance match

with the air. Fig. 2(b) shows the effect of substrate loss tangent on the reflection of the metasurface. The change of substrate loss tangent has little effect on the reflection of the metasurface. Therefore, to improve the simulation speed, the power loss density in Fig. 3 is simulated under the condition of $\tan\delta = 0$.

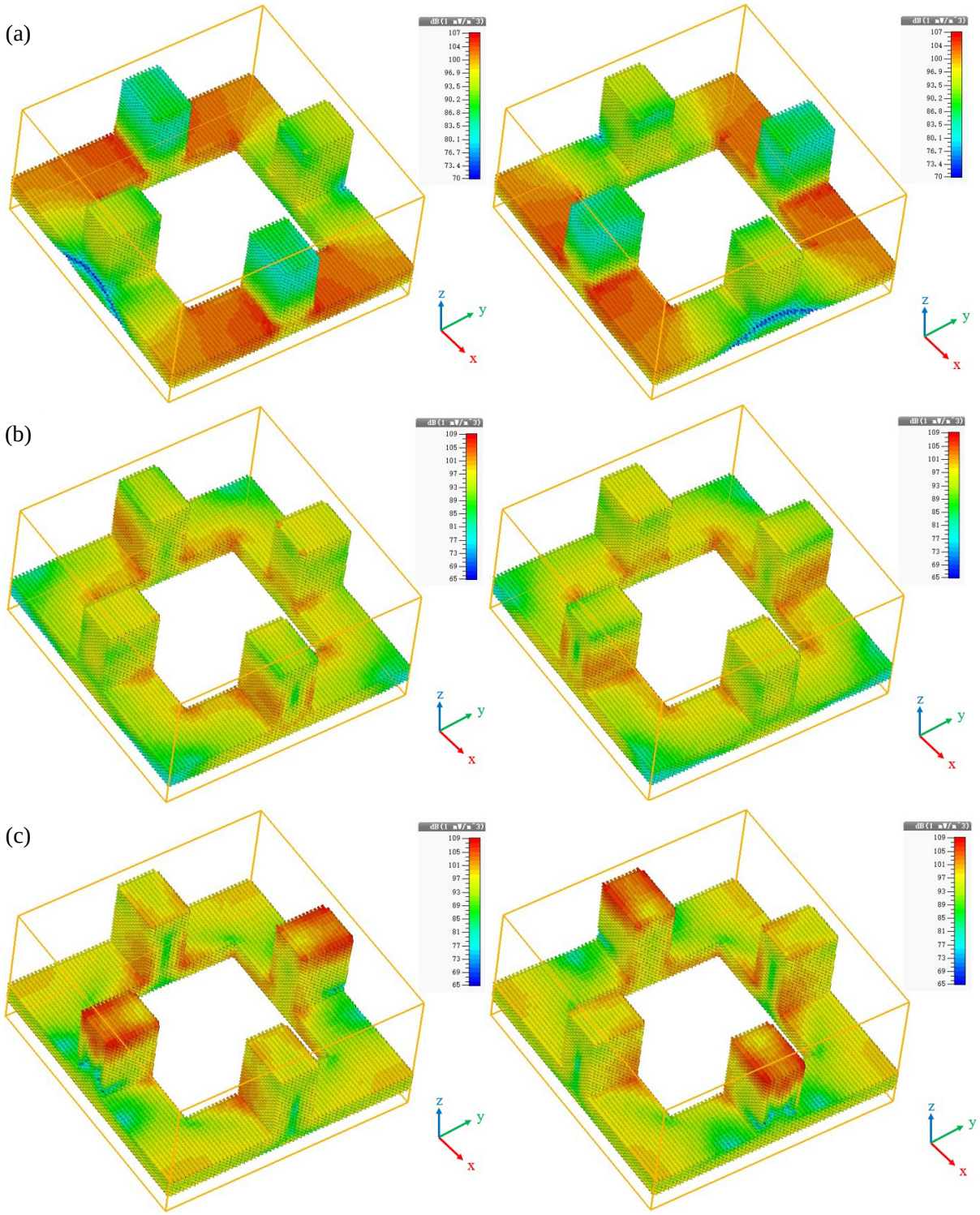

Figure 3. Power loss density at (a) 6.6 GHz, (b) 13 GHz and (c) 21.5 GHz.

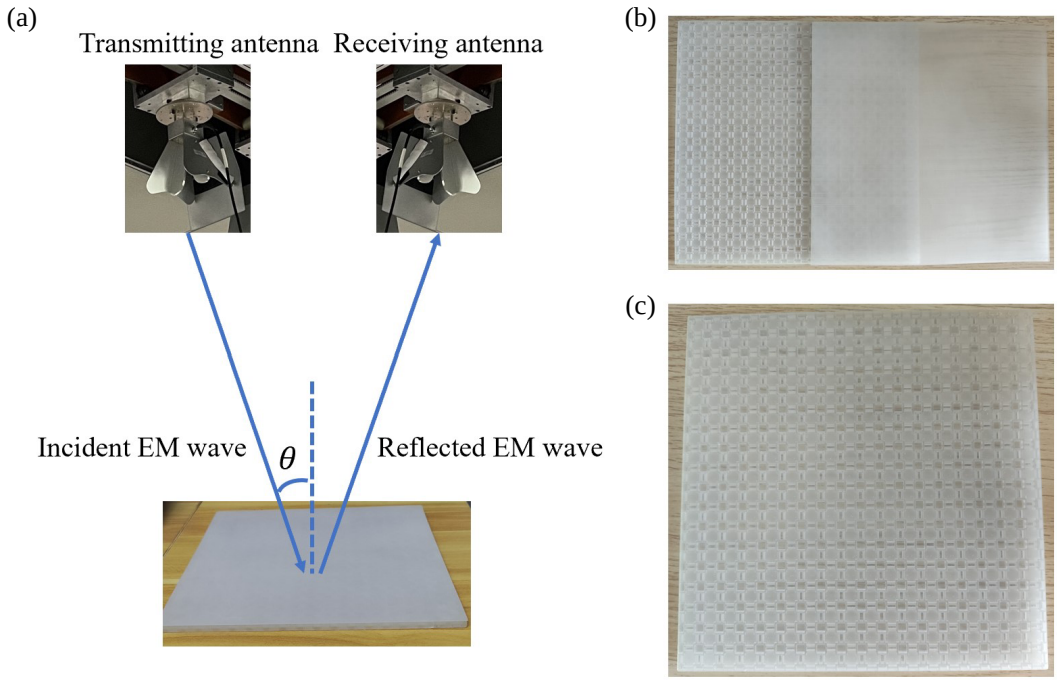

Figure 4. (a) The fabricated translucent water-based metasurface and experimental antenna. (b) The detachable top substrate. (c) Internal structure with removal of the top substrate.

4. RESULTS AND DISCUSSIONS

The translucent water-based metasurface, which is fabricated by 3D printing, consists of 18×18 elements with 10 mm period, and the total footprint of the absorbing metasurface is 180 mm $\times$ 180 mm, as shown in Fig. 4. Fig. 1(a) shows that the water resonant structure is connected to the air, so a baffle with 0.5 mm is added on the side of the metasurface to prevent water leakage. The top substrate of the translucent water-based metasurface is detachable to inject water into the metasurface, as shown in Fig. 4(b). When the water in the metasurface needs to be replaced, the top substrate is removed, and the water is poured out and sucked dry, then the required liquid can be refilled.

With a detachable top substrate, water with different conductivities can be injected into the metasurface. Three kinds of water with different conductivities are provided, and the conductivities are 0, 2388 μS/m, and 5377 μS/m, respectively. Fig. 5(a) shows the reflection of the metasurface in which water with three conductivities is injected. The resonant frequencies increase, and the reflection decreases with the increase of the conductivity of the injected water. Because of the increase of water conductivity, the absorption of water resonant structure to EM wave increases, and the broadband absorption of resonant frequency will become worse. However, with the increase of water conductivity, the lower bound of bandwidth does not increase with the increase of resonant frequency, while the upper bound of the bandwidth increases. Therefore, we conclude that the higher the conductivity of water is, the less reflection the metasurface is, which means the larger absorption.

In general, the EM wave does not incident vertically onto the metasurface, so the translucent water-based metasurface needs to realize a wide incident angle absorption in a wide bandwidth. Figs. 5(b)–(d) show the measured reflection spectra of the metasurface in which water with three conductivity is injected under a wide incident angle. Since the fabricated metasurface is geometrically symmetric, the measured results are independent of the polarization of the incident EM wave. In this paper, TE wave is used for measurement. With the increase of oblique incident angle, the distance between low and high resonant frequencies increases, and the reflection at high resonant frequency increases, which makes the reflection peak at 8 GHz increase and bandwidth narrow. However, the oblique incident angle has little effect on the lower bound of the bandwidth, so the translucent water-based metasurface can operate at

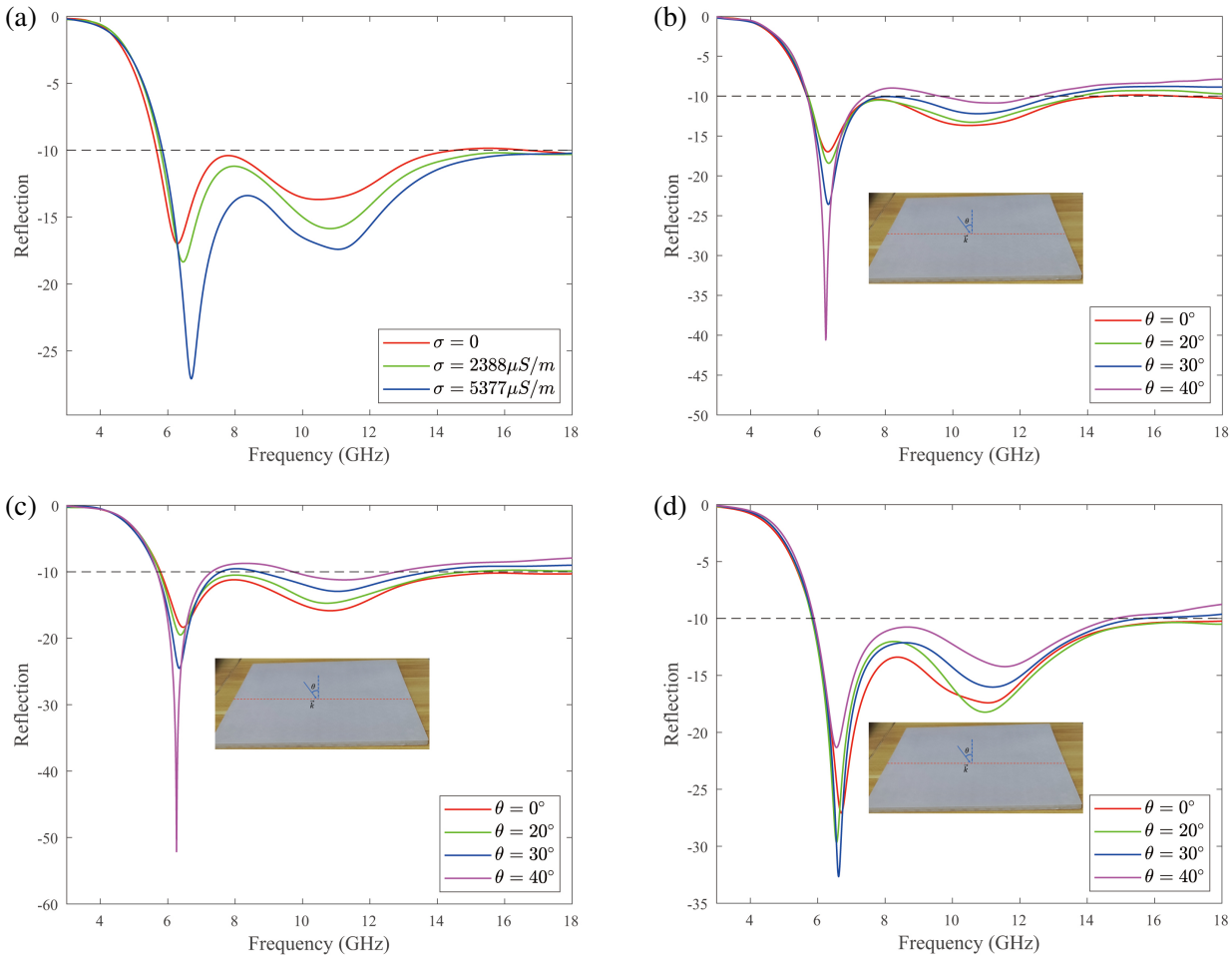

Figure 5. (a) Measured reflection spectra of the translucent water-based metasurface when the conductivity of injected water is 0, 2388 μS/m and 5377 μS/m. Measured reflection spectra of the translucent water-based metasurface under wide incident angle when the conductivity of injected water is (b) 0, (c) 2388 μS/m and (d) 5377 μS/m.

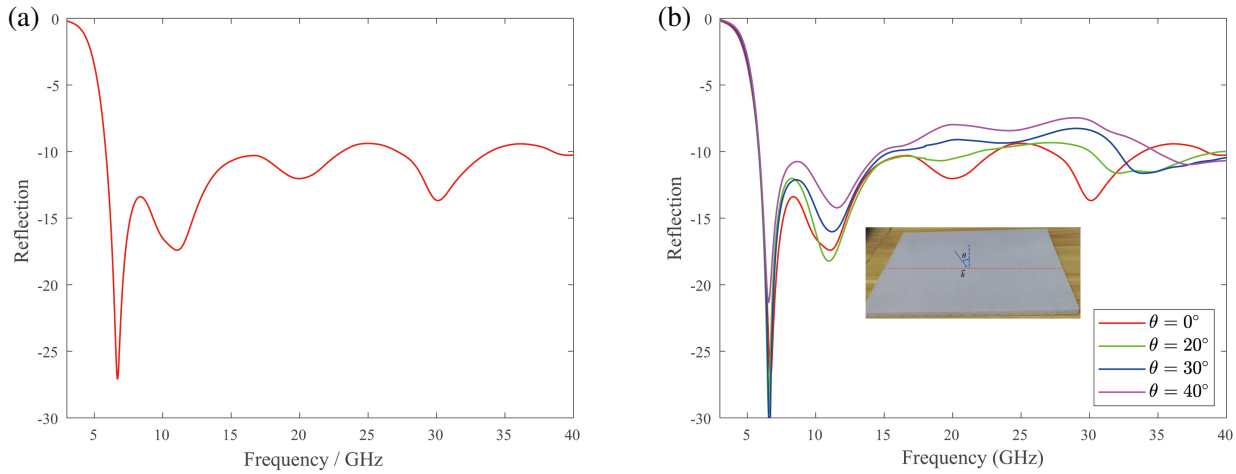

Figure 6. Measured reflection spectra of the translucent water-based metasurface when the conductivity of injected water is 5377 μS/m under (a) vertically incidence and (b) oblique incidence.

a wide incident angle when the conductivity of injected water is 5377 μS/m. Fig. 5(d) shows that the upper bound of the bandwidth exceeds 18 GHz when it is vertically incident. Thus, the reflection of the metasurface between 18 GHz and 40 GHz is measured. Fig. 6 shows the measured reflection spectra of the metasurface when the conductivity of injected water is 5377 μS/m. The reflection of the translucent water-based metasurface is less than −10 dB with frequency from 5.85 GHz to 23.1 GHz. Meanwhile, the low reflection and large bandwidth are also preserved when the oblique incident angle increases from 0° to 40°. Even if the incident angle is 40°, the bandwidth of the metasurface is from 5.85 GHz to 14.8 GHz.

5. CONCLUSION

A translucent water-based metasurface is proposed in this work. Firstly, the effect of water conductivity on the reflection of metasurface is studied. The experimental results are basically consistent with the simulation ones, when the conductivity of injected water is 5377 μS/m. The absorption of the translucent water-based metasurface is more than 90% with frequency from 5.85 GHz to 23.1 GHz. The bandwidth of the translucent water-based metasurface is broad and the realize high absorption within broad bandwidth with the incident angle from 0° to 40°. Due to the limited accuracy of the 3D printing instrument, the thickness of the metasurface is not very thin. However, with the development of 3D printing technology and polishing technology, metasurface thickness can be thinner and can be changed from translucent to transparent, which make it have a wider range of applications.

ACKNOWLEDGMENT

The work at Zhejiang University was sponsored by the Key Research and Development Program of the Ministry of Science and Technology under Grants No. 62071423 (to B. Z.), the Natural Science Foundation of Zhejiang Province under Grant LR23F010004 (to B. Z.), and the Top-Notch Young Talent of Zhejiang Province (to B. Z.).

Authors' contributions

B. Z conceived the idea and supervised the research. B. Z and M. H guided the theory, simulations and experiment. C. C. and T. C. performed the simulations and experimental verifications. C. C., T. C., M. H., H. L., B. Z. analyzed the data. C. C. wrote the paper. All authors discussed the results and commented on the manuscript.

Competing interests

The authors declare no competing financial interests.

REFERENCES

1. Duan, X., X. Chen, Y. Zhou, L. Zhou, and S. Hao, "Wideband metamaterial electromagnetic energy harvester with high capture efficiency and wide incident angle," *IEEE Antennas and Wireless Propagation Letters*, Vol. 17, No. 9, 1617–1621, 2018.
2. Shou, Y., Y. Feng, Y. Zhang, H. Chen, and H. Qian, "Deep learning approach based optical edge detection using ENZ layers," *Progress In Electromagnetics Research*, Vol. 175, 81–89, 2022.
3. Hu, Z., N. He, Y. Sun, Y. Jin, and S. He, "Wideband high-reflection chiral dielectric metasurface," *Progress In Electromagnetics Research*, Vol. 172, 51–60, 2021.
4. Huang, M., B. Zheng, T. Cai, X. Li, J. Liu, C. Qian, and H. Chen, "Machine-learning-enabled metasurface for direction of arrival estimation," *Nanophotonics*, Vol. 11, No. 9, 2001–2010, 2022.
5. Lu, H., J. Zhao, B. Zhen, C. Qian, T. Cai, E. Li, and H. Chen, "Eye accommodation-inspired neuro-metasurface focusing," *Nature Communications*, Vol. 14, No. 1, 3301, 2023.
6. Huang, H.-F. and H. Huang, "Millimeter-wave wideband high efficiency circular airy OAM multibeams with multiplexing OAM modes based on transmission metasurfaces," *Progress In Electromagnetics Research*, Vol. 173, 151–159, 2022.

7. Lu, H., B. Zheng, T. Cai, C. Qian, Y. Yang, Z. Wang, and H. Chen, "Frequency-controlled focusing using achromatic metasurface," *Advanced Optical Materials*, Vol. 9, No. 1, 2001311, 2021.
8. Hao, H., X. Ran, Y. Tang, S. Zheng, and W. Ruan, "A single-layer focusing metasurface based on induced magnetism," *Progress In Electromagnetics Research*, Vol. 172, 77–88, 2022.
9. Zheng, B., H. Lu, C. Qian, D. Ye, Y. Luo, and H. Chen, "Revealing the transformation invariance of full-parameter omnidirectional invisibility cloaks," *Electromagnetic Science*, Vol. 1, No. 2, 0020092, 2023.
10. Cai, T., B. Zheng, J. Lou, L. Shen, Y. Yang, S. Tang, E. Li, C. Qian, and H. Chen, "Experimental realization of a superdispersion-enabled ultrabroadband terahertz cloak," *Advanced Materials*, Vol. 34, No. 47, 2205053, 2022.
11. Tan, Q., B. Zheng, T. Cai, C. Qian, R. Zhu, X. Li, and H. Chen, "Broadband spin-locked metasurface retroreflector," *Advanced Science*, Vol. 9, No. 20, 2201397, 2022.
12. Singh, V. K., A. Shukla, M. K. Patra, L. Saini, R. K. Jani, S. R. Vadera, and N. Kumar, "Microwave absorbing properties of a thermally reduced graphene oxide/nitrile butadiene rubber composite," *Carbon*, Vol. 50, No. 6, 2202–2208, 2012.
13. Li, L., R. Xi, H. Liu, and Z. Lv, "Broadband polarization-independent and low-profile optically transparent metamaterial absorber," *Applied Physics Express*, Vol. 11, No. 5, 052001, 2018.
14. Schurig, D., J. J. Mock, B. J. Justice, S. A. Cummer, J. B. Pendry, A. F. Starr, and D. R. Smith, "Metamaterial electromagnetic cloak at microwave frequencies," *Science*, Vol. 314, No. 5801, 977–980, 2006.
15. Zhang, Y., Y. Huang, T. Zhang, H. Chang, P. Xiao, H. Chen, Z. Huang, and Y. Chen, "Broadband and tunable high-performance microwave absorption of an ultralight and highly compressible graphene foam," *Advanced Materials*, Vol. 27, No. 12, 2049–2053, 2015.
16. Fante, R. L. and M. T. McCormack, "Reflection properties of the salisbury screen," *IEEE Transactions on Antennas and Propagation*, Vol. 36, No. 10, 1443–1454, 1988.
17. Du Toit, L. J., "The design of jauman absorbers," *IEEE Antennas and Propagation Magazine*, Vol. 36, No. 6, 17–25, 1994.
18. Jaggard, D. L., N. Engheta, and J. Liu, "Chiroshield: A Salisbury/Dallenbach shield alternative," *Electronics Letters*, Vol. 26, No. 17, 1332–1334, 1990.
19. Li, S. J., P. X. Wu, H. X. Xu, Y. L. Zhou, X. Y. Cao, J. F. Han, C. Zhang, H. H. Yang, and Z. Zhang, "Ultra-wideband and polarization-insensitive perfect absorber using multilayer metamaterials, lumped resistors, and strong coupling effects," *Nanoscale Research Letters*, Vol. 13, No. 1, 386, 2018.
20. Hu, X., G. Xu, L. Wen, H. Wang, Y. Zhao, Y. Zhang, D. R. S. Cumming, and Q. Chen, "Metamaterial absorber integrated microfluidic terahertz sensors," *Laser & Photonics Reviews*, Vol. 10, No. 6, 962–969, 2016.
21. Park, S. J., S. A. N. Yoon, and Y. H. Ahn, "Dielectric constant measurements of thin films and liquids using terahertz metamaterials," *RSC Advances*, Vol. 6, No. 73, 69381–69386, 2016.
22. Ge, J., Y. Zhang, H. Li, H. Dong, and L. Zhang, "Ultra-broadband, tunable, and transparent microwave meta-absorber using ITO and water substrate," *Advanced Optical Materials*, Vol. 11, No. 10, 2202873, 2023.
23. Rybin, M. V., D. S. Filonov, K. B. Samusev, P. A. Belov, Y. S. Kivshar, and M. F. Limonov, "Phase diagram for the transition from photonic crystals to dielectric metamaterials," *Nature Communications*, Vol. 6, No. 1, 10102, 2015.
24. Odit, M., P. Kapitanova, A. Andryieuski, P. Belov, and A. V. Lavrinenko, "Experimental demonstration of water based tunable metasurface," *Applied Physics Letters*, Vol. 109, No. 1, 011901, 2016.
25. Feng, M., X. Tian, J. Wang, M. Yin, S. Qu, and D. Li, "Broadband abnormal reflection based on a metal-backed gradient index liquid slab: An alternative to metasurfaces," *Journal of Physics D: Applied Physics*, Vol. 48, No. 24, 245501, 2015.

26. Tiwari, P. and S. K. Pathak, "Design and simulation of a water based polarization-insensitive and wide incidence dielectric metasurface absorber for X-, Ku- and K-band," *2021 IEEE Indian Conference on Antennas and Propagation*, 692–695, 2021.
27. Tan, X., J. Chen, J. Li, and S. Yan, "Water-based metasurface with continuously tunable reflection amplitude," *Journal of Physics D: Applied Physics*, Vol. 30, No. 5, 6991–6998, 2022.
28. Kim, H. K., D. Lee, and S. Lim, "A fluidically tunable metasurface absorber for flexible large-scalewireless ethanol sensor applications," *Sensors*, Vol. 16, No. 8, 1246, 2016.
29. Kim, H. K., D. Lee, and S. Lim, "Wideband-switchable metamaterial absorber using injected liquid metal," *Scientific Reports*, Vol. 6, No. 1, 31823, 2016.
30. Minovich, A., J. Farnell, D. N. Neshev, et al., "Liquid crystal based nonlinear fishnet metamaterials," *Applied Physics Letters*, Vol. 100, No. 12, 121113, 2012.
31. Andryieuski, A., S. M. Kuznetsova, S. V. Zhukovsky, Y. S. Kivshar, and A. V. Lavrinenko, "Water: Promising opportunities for tunable all-dielectric electromagnetic metamaterials," *Scientific Reports*, Vol. 5, No. 1, 13535, 2015.
32. Yoo, Y. J., S. Ju, S. Y. Park, Y. J. Kim, J. Bong, T. Lim, K. W. Kim, J. Y. Rhee, and Y. Lee, "Metamaterial absorber for electromagnetic waves in periodic water droplets," *Scientific Reports*, Vol. 5, No. 1, 14018, 2015.
33. Song, Q., W. Zhang, P. C. Wu, et al., "Water-resonator-based metasurface: An ultrabroadband and near-unity absorption," *Advanced Optical Materials*, Vol. 5, No. 8, 1601103, 2017.
34. Su, J., Y. Li, M. Qu, H. Yu, Q. Guo, and Z. Li, "A 3-D-printed ultrawideband and ultralow-scattering water-based metasurface," *IEEE Transactions on Antennas and Propagation*, Vol. 71, No. 3, 2885–2890, 2023.
35. Chen, W., H. Liu, Y. Jia, Y. Liu, and X. Wang, "Ultra-wideband low-scattering metamaterial based on combination of water absorber and polarization rotation metasurface," *International Journal of RF and Microwave Computer-Aided Engineering*, Vol. 32, No. 9, e23260, 2022.
36. Wen, J., Q. Ren, R. Peng, and Q. Zhao, "Multi-functional tunable ultra-broadband water-based metasurface absorber with high reconfigurability," *Journal of Physics D: Applied Physics*, Vol. 55, No. 28, 285103, 2022.
37. Shen, Y., J. Zhang, Y. Pang, L. Zheng, J. Wang, H. Ma, and S. Qu, "Thermally tunable ultra-wideband metamaterial absorbers based on three-dimensional water-substrate construction," *Scientific Reports*, Vol. 8, No. 1, 4423, 2018.
38. Xie, J., W. Zhu, I. V. Rukhlenko, F. Xiao, C. He, J. Geng, X. Liang, R. Jin, and M. Premaratne, "Water metamaterial for ultra-broadband and wide-angle absorption," *Optics Express*, Vol. 26, No. 4, 5052–5059, 2018.
39. Huang, X., H. Yang, Z. Shen, J. Chen, H. Lin, and Z. Yu, "Water-injected all-dielectric ultra-wideband and prominent oblique incidence metamaterial absorber in microwave regime," *Journal of Physics D: Applied Physics*, Vol. 50, No. 38, 385304, 2017.
40. Li, L., J. Wen, Y. Wang, Y. Jin, Y. Wen, J. Sun, Q. Zhao, B. Li, and J. Zhou, "A transparent broadband all-dielectric water-based metamaterial absorber based on laser cutting," *Physica Scripta*, Vol. 98, No. 5, 55516, 2023.
41. Zhao, J., S. Wei, C. Wang, K. Chen, B. Zhu, T. Jiang, and Y. Feng, "Broadband microwave absorption utilizing water-based metamaterial structures," *Optics Express*, Vol. 26, No. 7, 8522–8531, 2018.